PAPER

Study the optical properties of Pr_2CuO_4 thin films with different T_{c0} via spectroscopic ellipsometry

View the article online for updates and enhancements.

IOP ebooks™

Bringing you innovative digital publishing with leading voices to create your essential collection of books in STEM research.

Start exploring the collection - download the first chapter of every title for free.

Materials Research Express

PAPER

Study the optical properties of Pr_2CuO_4 thin films with different T_{c0} via spectroscopic ellipsometry

Yujun Shi[1], Jie Lian[1] , Xinjian Wei[2], Kui Jin[2] , Haonan Song[1], Mingyang Wei[1], Kai Dai[1], Qingfen Jiang[1] and Jiaxiong Fang[3]

[1] School of Information Science and Engineering, and Shandong Provincial Key Laboratory of Laser Technology and Application, Shandong University, Qingdao 266237, People's Republic of China
[2] Institute of Physics, Chinese Academy of Sciences, Beijing 100190, People's Republic of China
[3] Advanced Research Center for Optics, Shandong University, Jinan 250100, People's Republic of China

E-mail: jieliansdu@163.com

Abstract

In this work, we primarily present spectroscopic ellipsometry (SE) study on Pr_2CuO_4 (PCO) thin films, a parent compound of electron-doped cuprate superconductors. The c-aixs orientation films with various superconducting transition temperature T_{c0} were prepared by a chemical method, which are single phase and good crystallinity verified by x-ray diffraction. The imaginary part of dielectric function (ε_i) of PCO was investigated by SE using a four-layer optical model in the photon energy range from 1.55 to 4.13 eV. Through fitting the second derivative spectra of ε_i via critical point model, we find that the charge-transfer gap exists in PCO system and, more importantly, this gap has a negative relationship with T_{c0}. This viewpoint demonstrates that the charge-transfer gap would merge together with the electrons doping in PCO and opens a door to understand the nature of cuprate superconductors.

1. Introduction

The materials with the formula of RE_2CuO_4 (RE=rare earth ions) are the parent compounds of cuprate high transition temperature (high-T_c) superconductors. It is commonly accepted that superconductivity in parent compounds emerges after doping holes to T-phase with the Cu–O octahedra (formed by six oxygen atoms surrounding one copper atom) or doping electrons to T′-phase with the Cu–O square (formed by four oxygen atoms surrounding one copper atom), respectively [1]. For T′-phase, cation substitution has been long considered as the only way to prepare electron-doped superconductors. However, in 2008, Matsumoto *et al* reported that the superconductivity in parent compounds of electron-doped cuprates was achieved without any cation substitution [2]. This discovery may redraw the phase diagram and pave a way for uncovering the mechanism of high-T_c superconductors.

The parent compounds of cuprates are believed to belong to a class of materials known as charge-transfer insulators (or Mott insulators) [3]. The materials, which are predicted to be metallic by band theory, are actually insulators due to the Coulomb repulsion [4]. Cu-$d_{x^2-y^2}$ orbital level is split effectively into the upper and lower Hubbard bands by a correlation energy U. When O-2p band locates between U, the gap of O-2p band to upper Hubbard band is indicated to charge-transfer gap [5]. In 2002, Armitage *et al* revealed the charge-transfer band for the first time by Angle-Resolved Photoemission Spectroscopy [4]. However, how the charge-transfer gap or band change with doping electrons in parent compounds with superconductivity remain actively discussed.

Optical measurements can offer not only the low-lying intraband transition, but also the interband transitions from occupied to unoccupied states, thus it has been become a powerful tool to research the charge-transfer gap. In 2006, Wang *et al* demonatrated that the chemical potential moves into the conduction band as the $Nd_{2-x}Ce_xCuO_4$ ($0 \leqslant x \leqslant 0.20$) single crystal is doped by electrons by optical reflectivity [6]. In 2010, Pisarev *et al* invistigated the complex optical dielectric function ($\varepsilon = \varepsilon_r + i\varepsilon_i$) in several kinds of parent compounds of electron-doped cuprates and obtained the electric-dipole-allowed charge-transfer gap values by spectroscopic ellipsometry (SE) method [7]. However, the samples in previous expriments are not focus on the parent

compounds with superconductivity, which may lead to the fact that the conclusions are indirect and incomplete in somewhat. Moreover, as a nondestructive and accurate optical method, SE can measure the amplitude and phase information simultaneously [8] and has become a suitable way to determine the complex dielectric function for kinds of materials [9–12]. Therefore, in this work, the charge-transfer gap of parent compounds Pr_2CuO_4 (PCO) with superconductivity are studied by SE, which can provide the direct evidence for that how the charge-transfer gap vary with doping electrons in parent compound PCO system.

PCO thin films with different T_{c0} were synthesized by polymer assisted deposition (PAD) method. X-ray diffraction (XRD) was used to characterize lattice struture and c-aixs lattice constant, and atomic force microscope (AFM) offers the roughness layer information for SE data analysis. SE was employed to investigate PCO samples' dielectric functions, and critical point (CP) model was used to obtain the charge-transfer gap value for PCO thin films through fitting the second derivative spectra of ε_i. We find the gap values decrease as the T_{c0} increases. This phenomenon declears that the band structure would move and merge together as the electrons doping in PCO system. Therefore, we provide a possible way to uncover the mechanism of the superconductivity in parent compounds.

2. Experimental method

2.1. Materials
PCO thin films were grown on (00l)-orientation $SrTiO_3$ (STO) substrates by PAD method. In the precursor polymer solution, Pr and Cu nitrates offer the metal ion and were mixed at a certain stoichiometric. The organic polymer compounds are from polyethylenimine and ethylenediaminetetraacetic acid. Then, the precursor solution was spin coated on STO substrates. To decompose the polymer, the films were heated from room temperature to 550 °C in the air. The uncrystallized samples were crystallized and sintered at 850 °C under 200 Pa oxygen pressure in a tubular furnace for one hour. In the last, the PCO thin films were annealed about 1 Pa at various temperature. The more details about the film growth were documented in [13].

2.2. Methods
Resistivity was measured by a standard four-probe method using physical property measurement system (PPMS). The crystallization and surface morphology were characterized by XRD (Rigaku SmartLab9KW) and AFM (NaioAFM), repectively. SE (Sopra GES-5) was utilized to explore dielectric function in the photon energy range from 1.55 to 4.13 eV at 75° incidence. XRD, AFM and SE were all tested at room temperature (300 K). Samples with $T_{c0} = 22.7$ K (named as SC22), 15.3 K (SC15) and a non-superconduting (NSC) were carried out.

3. Experimental results and discussion

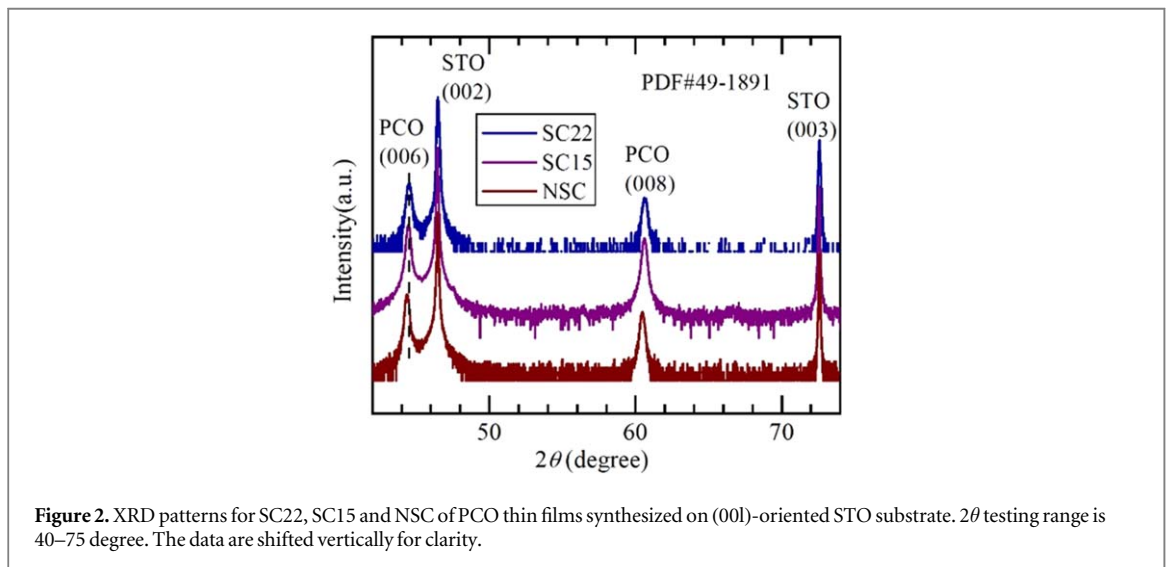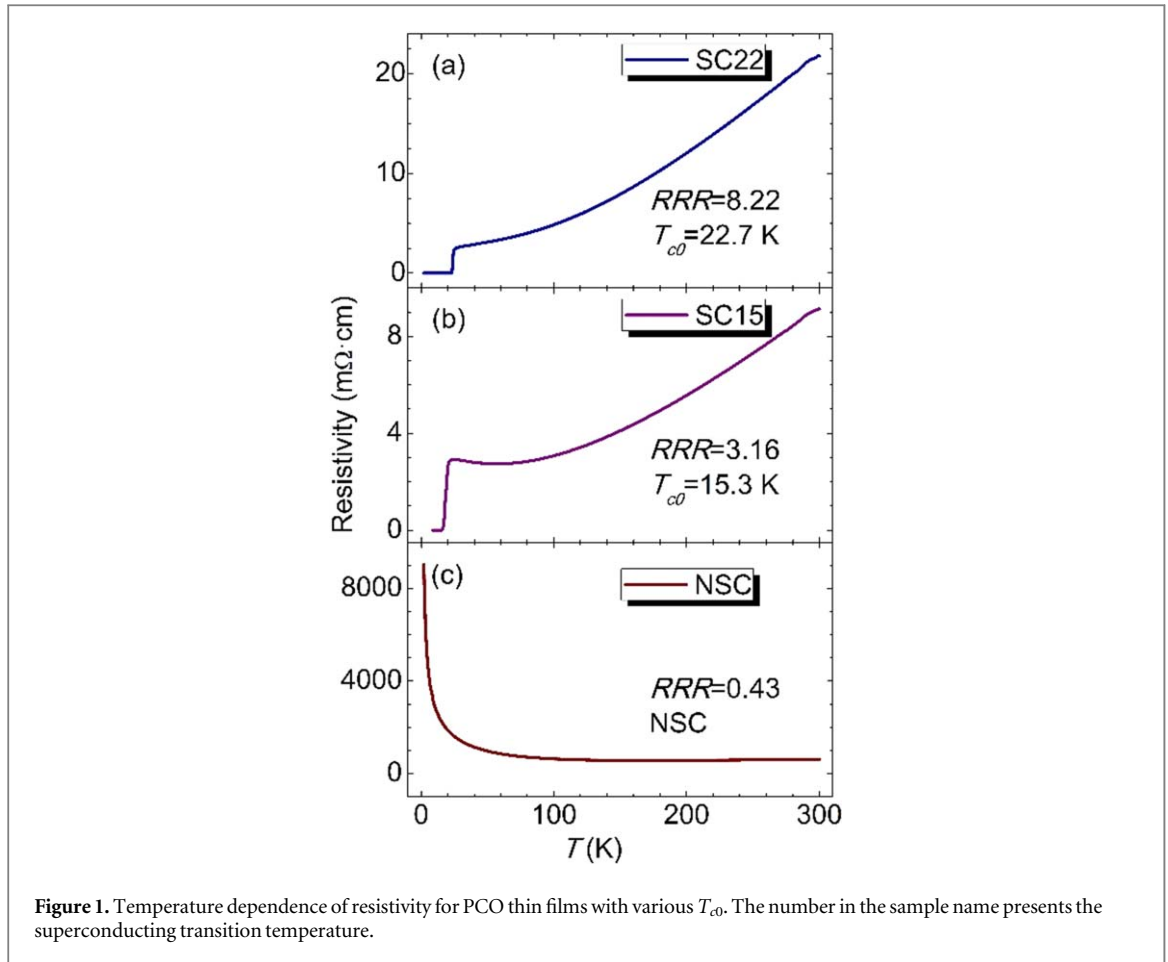### 3.1. Temperature dependence of resistivity measurement
Figures 1(a)–(c) show the temperature dependence of the resistivity for SC22, SC15 and NSC. For figures 1(a) and (b), the values of resistivity decrease monotonically with decreasing temperature down to $T_{c0} = 22$ K and 15 K, and the width of the superconducting transition is 1.67 K and 2.92 K for SC22 and SC15, respectively. However, the resistivity of NSC sample increases monotonically with decreasing temperature and shows the insulator property. *RRR* is defined as the residual resistance ratio by $R(300 \text{ K})/R(30 \text{ K})$, which equals to 8.22, 3.16 and 0.43 for SC22, SC15 and NSC, respectively. The values of *RRR* are in agreement with He *et al* work on tunneling study of PCO films [14]. Due to the fact that the amount of impurities and crystallographic defects can make the value of *RRR* decrease, thus, non-superconducting sample has more disorder than superconducting samples. In electron-doped cuprates, these defects mainly come from the apical oxygen and in-plane oxygen vacancies induced by under- or over-annealing process [14–16].

3.2. Crystal structure
To characterize the structure of PCO thin films, $\theta/2\theta$ was measured, as seen in figure 2. The card number for XRD is PDF#49-1891. All PCO peaks on STO (00 l) are sharp, indicating that the films show a single phase and *c*-axis orientation with good crystallinity. (006) diffraction peaks shifted to lower angle from SC22 to NSC stems from variation of *c*-axis lattice constants which could be calculated by Bragg's formula. The results show that the lattice constants relating with apical oxygen contents are 12.199 Å, 12.209 Å and 12.235 Å for SC22, SC15 and NSC, respectively, which is similar to Matsumoto *et al* work [17].

3.3. Surface topography
AFM is a sufficient method to analyze the surface morphology and roughness of thin films, and the 3D graphs of SC22, SC15 and NSC are shown in figures 3(a)–(c). The testing area is 1 μm × 1 μm and the size of swells

Figure 1. Temperature dependence of resistivity for PCO thin films with various T_{c0}. The number in the sample name presents the superconducting transition temperature.

Figure 2. XRD patterns for SC22, SC15 and NSC of PCO thin films synthesized on (00l)-oriented STO substrate. 2θ testing range is 40–75 degree. The data are shifted vertically for clarity.

decreases as superconducting transition temperature increase. Based on this measuring results, roughness layer should be added in the SE optical model owing to surface sensitivity.

3.4. Spectroscopic ellipsometry
In SE experiment, the relevant measured quantities are tanΨ and cosΔ which describe the change of polarization state upon reflection, called complex reflectance ratio ρ:

$$\rho = \frac{\chi_i}{\chi_r} = \tan\Psi e^{i\Delta} \tag{1}$$
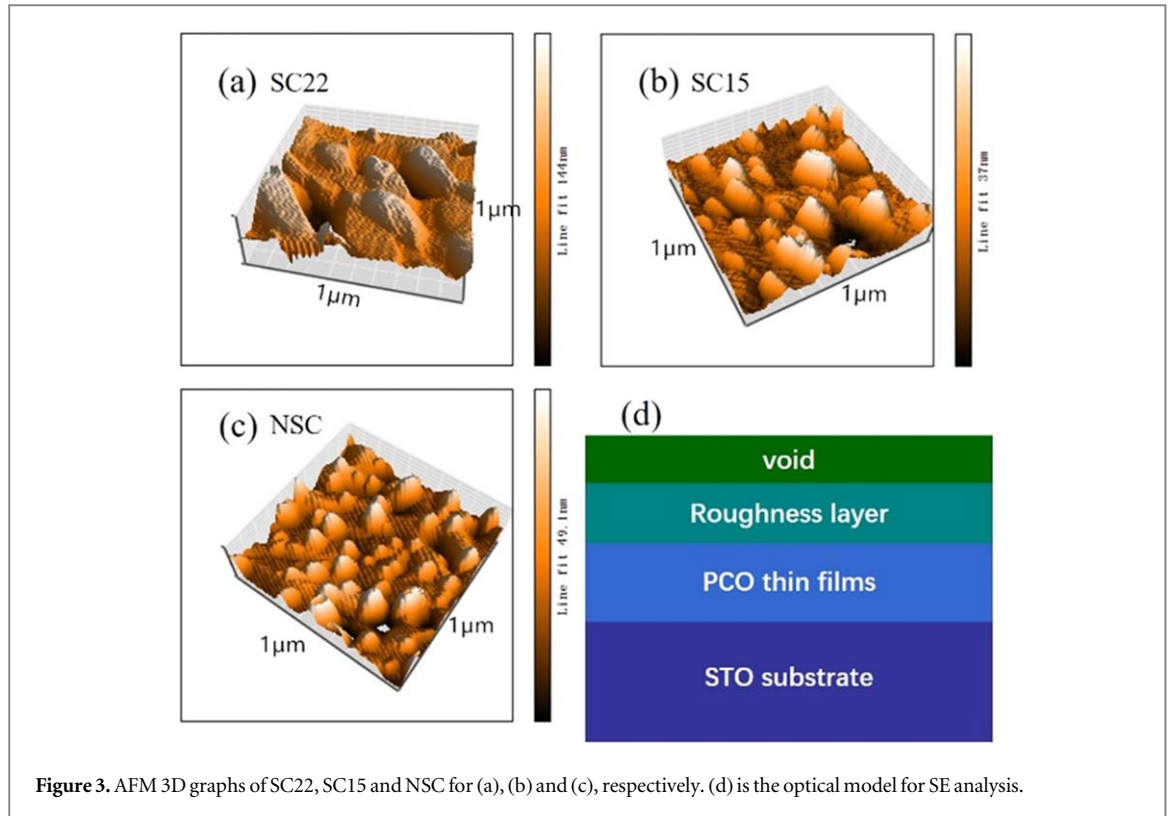
Figure 3. AFM 3D graphs of SC22, SC15 and NSC for (a), (b) and (c), respectively. (d) is the optical model for SE analysis.

where χ_i and χ_r are the incident and reflected light polarization states, respectively [18]. Figure 4 exhibits the experimental (grey solid lines) and simulated (dot lines) results of $\tan\Psi$ and $\cos\Delta$ for PCO thin films. Because SE is a surface sensitive technique, a four-layer optical structure should be built according to AFM results, that is air/surface roughness/PCO/STO-substrate (see figure 3(d)). We consider air as the first layer. Surface roughness as the second layer is modeled by Bruggeman effective-medium approximation with a mixture of the material (50%) and voids (50%), and the thickness of roughness is offered by AFM. PCO as the third layer is described by Drude and two Lorentz oscillators dispersion. Because equation (1) is a nonlinear transcendental equation, inversion method is commonly taken into account to treat after measurement data acquisition [19]. Thus, an evaluation function should be added to determine the goodness of the optical model, and usually defined via the lowest mean squared error (MSE) [20]:

$$MSE = \frac{1}{2n-m-1}\sum_{i=1}^{n}[(\tan\Psi_{cal}^{i} - \tan\Psi_{exp}^{i})^2 + (\cos\Delta_{cal}^{i} - \cos\Delta_{exp}^{i})^2] \qquad (2)$$

where n is the number of measured Ψ and Δ, m is the number of fit parameters and, cal and exp represent to theoretically calculated data and experimentally measured data, respectively. Through fitting the parameters of Drude and Lorentz dispersion laws, a favorable agreement between simulation and experiment was obtained and showed in figure 4, and the relatively small MSE values are listed in table 1.

Finally, the imaginary part of dielectric functions (ε_i) of PCO are extracted from the optical model as shown in figures 5(a)–(c), respectively. We find that the Drude contribution remarked by diagonal lines gradually decreases as T_{c0} decreasing, indicating that metal property of PCO decreases in room temperature.
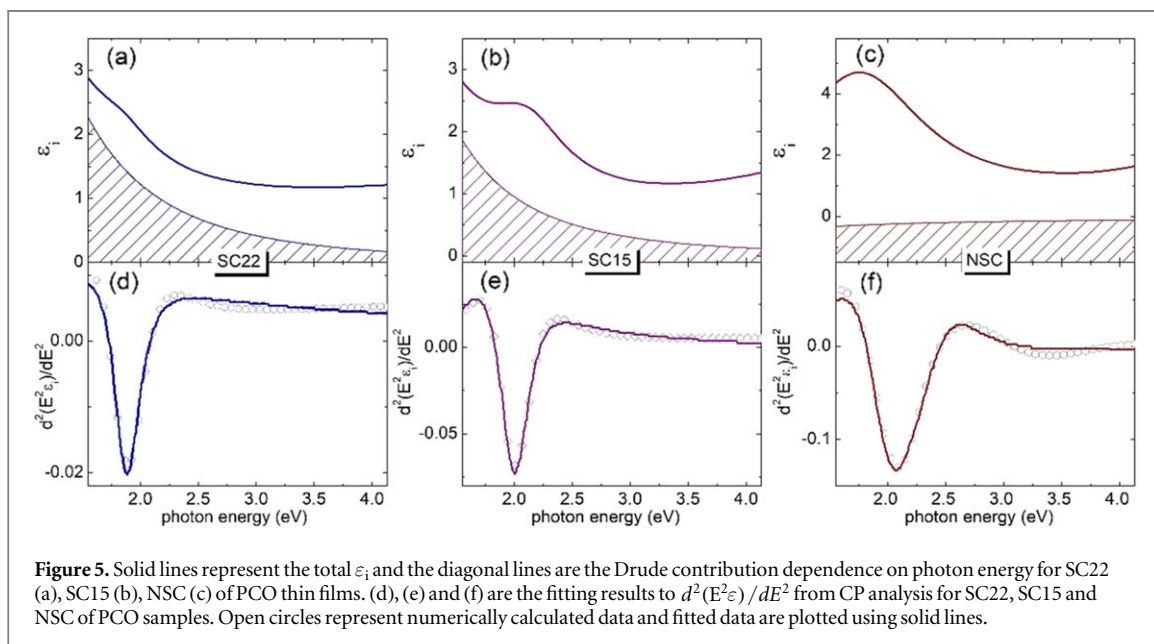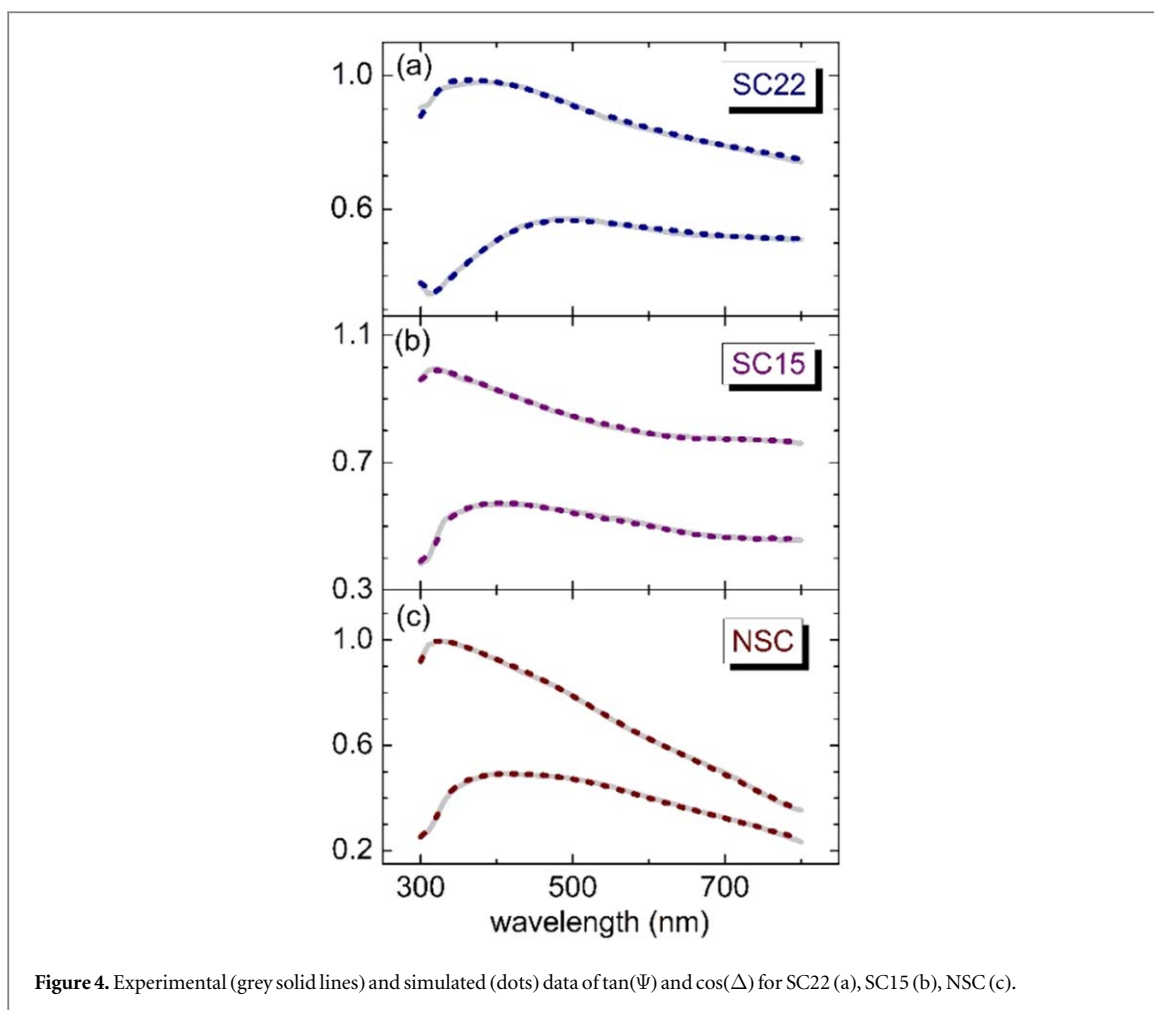
When the dielectric functions are extracted by mathematical inversion, the band structures of material can be evaluated by a CP analysis which is performed by fitting second derivative spectra of $\varepsilon(E)$ since it becomes zero in a region where the dielectric function varies smoothly [21]. The equations are expressed as follows [22]:

$$\frac{d^2(E^2\varepsilon)}{dE^2} = \begin{cases} n(n-1)A_m e^{i\varphi_m}(E - E_{cp} + i\Gamma_m)^{n-2} & n \neq 0 \\ A_m e^{i\varphi_m}(E - E_{cp} + i\Gamma_m)^{-2} & n = 0 \end{cases} \qquad (3)$$
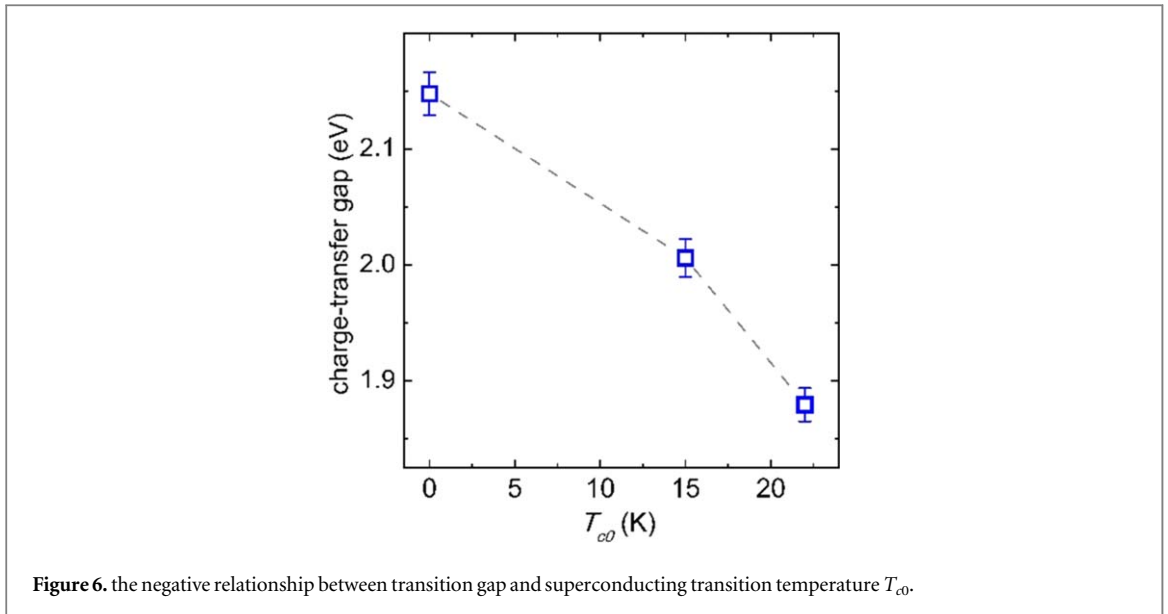
In CP analysis, (A, E_{cp}, Γ, φ) are fitted as analysis parameters, where represent the amplitude parameter, energy of threshold, broadening and excitonic angle, respectively. In our work, we choose n = 1/2 and ε_r and ε_i were simultaneously fitted whereas. The calculated and simulated spectra are exhibited in figures 5(d)–(f) for SC22, SC15 and NSC of PCO samples. The obtained E_{cp} and fitting parameters derived from the CP model are listed in table 2.

3.5. Band gap of PCO

From table 2, the E_{cp} values are 1.87, 2.00 and 2.14 eV for SC22, SC15 and NSC, respectively. As a possibility, one may suspect that the gap results from the crystal field *d-d* transitions between 3d levels split by the crystal field in the photon

Figure 4. Experimental (grey solid lines) and simulated (dots) data of tan(Ψ) and cos(Δ) for SC22 (a), SC15 (b), NSC (c).

Figure 5. Solid lines represent the total ε_i and the diagonal lines are the Drude contribution dependence on photon energy for SC22 (a), SC15 (b), NSC (c) of PCO thin films. (d), (e) and (f) are the fitting results to $d^2(\mathrm{E}^2\varepsilon)/dE^2$ from CP analysis for SC22, SC15 and NSC of PCO samples. Open circles represent numerically calculated data and fitted data are plotted using solid lines.

Table 1. MSE values.

sample	SC22	SC15	NSC
MSE (10^{-4})	4.68	6.49	6.43

Figure 6. the negative relationship between transition gap and superconducting transition temperature T_{c0}.

Table 2. the parameters of the standard critical point model.

Sample	A_m	E_{cp} (eV)	Γ_m (eV)	φ_m (deg.)
SC22	0.0029	1.8794	0.1784	126.1060
SC15	0.0120	2.006	0.1935	137.2139
NSC	0.0243	2.1476	0.3917	278.2671

energy of 1.4–2.4 eV. However, the forbidden *d-d* transitions are too weak to be detected in ellipsometry because it is sensitive to strong transitions [7]. In other research, it has been reported that the gap can be attributed to interband transition in high energy range (visible region) [1]. Thus, the behavior of intense transition could be assigned to charge-transfer gap, which has been studied by optical measurement [5–7, 23]. As mentioned above, the charge-transfer gap represents the transition between O-2p band to upper Hubbard band which is formed by the Cu $d_{x^2-y^2}$-orbital band split because of the strong on-site coulomb repulsion effect [3, 24, 25]. As early as 1990, Tokura *et al* pointed out the charge-transfer gap exists positive correlation with the number of apical oxygens [23]. In our work, we find that superconducting transition temperature has negative correlation with the charge-transfer gap for PCO, which is consistent with Wang *et al*, see figure 6. Uncovering this issue may plays a significant role to understand parent compounds.

To disclose this phenomenon, apical oxygen contents should be considered because the apical oxygens play a strong scattering center role in electron-doped cuprate superconductors [26]. As mentioned in XRD results, the *c*-axis lattice constants are 12.199 Å, 12.209 Å and 12.235 Å for SC22, SC15 and NSC. Very recently, Wei *et al* utilized electrical transport measurement to explore the intrinsic electronic state of PCO and declared that removing oxygens is equal to introduce electrons, which is similar to dope Ce into system [13]. Therefore, according to the *c*-axis lattice constants, it is evidential to view different T_{c0} as different doping electrons concentration in this work.

The reason why the superconducting transition temperature has negative correlation with the charge-transfer gap for PCO can be looked at the electronic states of the Cu-O planes which control the physics of cuprate high-T_c superconductors. On the one hand, the introduced electrons in PCO occupy the states of Cu-3d level, which equals to plus an effective potential to O-2p level. On the other hand, the effect of electrostatic screening increases as the electrons increase, which leads to the on-site Coulomb interaction decreases among Cu-3d electrons [27]. Therefore, the experimental phenomenon can be stemmed from the raising of O-2p level and declining of upper Hubbard band, indicating that the O-2p level and upper Hubbard band would be merged together as doping electrons into PCO. This scenario is clearer to directly explore the relationship of charge-transfer gap with the parent compound PCO with different T_{c0}.

4. Conclusions

In summary, SE technique, as an accurate and non-destructive optical detection method, allows us to explore the charge-transfer gap value for the parent compound of PCO thin films with various T_{c0}. More importantly, we find

that the charge-transfer gap has a negative correlation with T_{c0}. This phenomenon is related to the fact that O-2p band moves toward the upper Hubbard band due to electrons doping into PCO system. In this case, we firstly show this result and directly provide a new insight for understand the nature of the cuprate high-T_c superconductors.

Acknowledgments

ORCID iDs

Jie Lian   https://orcid.org/0000-0001-5269-3193
Kui Jin   https://orcid.org/0000-0003-2208-8501

References

[1] Chanda G, Lobo R P S M, Schachinger E, Wosnitza J, Naito M and Pronin A V 2014 Optical study of superconducting Pr_2CuO_x with $x \simeq 4$ *Phys. Rev.* B **90** 024503

[2] Matsumoto O, Utsuki A, Tsukada A, Yamamoto H, Manabe T and Naito M 2008 Superconductivity in undoped T'-RE_2CuO_4 with T_c over 30 K *Physica* C **468** 1148–51

[3] Damascelli A, Hussain Z and Shen Z X 2003 Angle-resolved photoemission studies of the cuprate superconductors *Rev. Mod. Phys.* **75** 473–541

[4] Armitage N P *et al* 2002 Doping dependence of an n-type cuprate superconductor investigated by angle-resolved photoemission spectroscopy *Phys. Rev. Lett.* **88** 257001-1

[5] Arima T, Kikuchi K, Kasuya M, Koshihara S, Tokura Y, Ido T and Uchida S 1991 Optical excitations in CuO_2 sheets and their strong dependence on Cu–O coordination and bond length *Phys. Rev.* B **44** 917–20

[6] Wang N L, Li G, Wu D, Chen X H, Wang C H and Ding H 2006 Doping evolution of the chemical potential spincorrelation gap and charge dynamics of $Nd_{2-x}Ce_xCuO_4$ *Phys. Rev.* B **73** 184502

[7] Pisarev R V, Pavlov V V, Kalashnikova A M and Moskvin A S 2010 Near-band gap electronic structure of the tetragonal rare-earth cuprates R_2CuO_4 and the bismuth cuprate Bi_2CuO_4 *Phys. Rev.* B **82** 224502

[8] Shi Y J, Lian J, Hu W, Liu Y X, He G, Jin K, Song H N, Dai K and Fang J X 2019 Study the relation between band gap value and lattice constant of $MgTi_2O_4$ *J. Alloys Compd.* **788** 891–6

[9] Diware M S, Ganorkar S P, Park K, Chegal W, Cho H M, Cho Y J, Kim Y D and Kim H 2018 Dielectric function, critical points, and Rydberg exciton series of WSe_2 monolayer *J. Phys. Condens. Mat.* **30** 235701

[10] Halim J, Persson I, Moon E J, Kuhne P, Darakchieva V, Persson P O A, Eklund P, Rosen J and Barsoum M W 2019 Electronic and optical characterization of 2D Ti_2C and Nb_2C (MXene) *thin films J. Phys. Condens. Mat.* **31** 165301

[11] Xie Z, Sun S, Yan Y, Zhang L, Hou R, Tian F and Qin G G 2017 Refractive index and extinction coefficient of $NH_2CH = NH_2PbI_3$ perovskite photovoltaic material *J. Phys. Condens. Mat.* **29** 245702

[12] Mahmood A, Aziz U, Rashid R, Shah A, Ali Z, Raza Q, Raffi M and Shakir I 2014 Exploration of optical behavior of $Cd_{1-x}Ni_xTe$ thin films by spectroscopic ellipsometry *Mater. Res. Express* **1** 046409-1

[13] Wei X J, He G, Hu W, Zhang X, Qin M Y, Yuan J, Zhu B Y, Lin Y and Jin K 2019 Tunable superconductivity in parent cuprate $Pr_2CuO_{4 \pm \delta}$ thin films *Chin. Phys.* B **28**

[14] He G, Wei X J, Zhang X, Shan L, Yuan J, Zhu B Y, Lin Y and Jin K 2017 Normal-state gap in the parent cuprate $Pr_2CuO_{4 \pm \delta}$ *Phys. Rev.* B **96** 104518

[15] Radaelli P G, Jorgensen J D, Schultz A J, Peng J L and Greene R L 1994 Evidence of apical oxygen inNd_2CuOdetermined by single-crystal neutron diffraction *Phys. Rev.* B **49** 15322–15326

[16] Higgins J S, Dagan Y, Barr M C, Weaver B D and Greene R L 2006 Role of oxygen in the electron-doped superconducting cuprates *Phys. Rev.* B **73** 104510

[17] Matsumoto O, Utsuki A, Tsukada A, Yamamoto H, Manabe T and Naito M 2009 Synthesis and properties of superconducting$T'-R_2CuO_4(R = Pr, Nd, Sm, Eu, Gd)$ *Phys. Rev.* B **79** 100508

[18] Alonso M I, Tortosa S, Garriga M and Pinol S 1997 Ellipsometric measurement of the dielectric tensor of $Nd_{2-x}Ce_xCuO_{4-delta}$ *Phys. Rev.* B **55** 3216–21

[19] Sun Z, Lian J, Gao S, Wang X, Wang Y and Yu X 2014 Complex refractive index and thickness characterization based on ant colony algorithm and comprehensive evaluation function *J. Comput. Theor. Nanos* **11** 816–20

[20] Zhao M L, Lian J, Yu H S, Jin K, Xu L P, Hu Z G, Yang X L and Kang S S 2017 Dielectric functions of La-based cuprate superconductors for visible and near-infrared wavelengths *Appl. Surf. Sci.* **421** 611–6

[21] Fujiwara H 2007 *Spectroscopic Ellipsometry: Principles and Applications* ed J Wiley, 7, p 388(Tokyo, Japan: Maruzen Co. Ltd)

[22] Jiang Y J, Soufiani A M, Gentle A, Huang F Z, Ho-Baillie A and Green M A 2016 Temperature dependent optical properties of $CH_3NH_3PbI_3$ perovskite by spectroscopic ellipsometry *Appl. Phys. Lett.* **108** 061905

[23] Tokura Y, Koshihara S, Arima T, Takagi H, Ishibashi S, Ido T and Uchida S 1990 Cu-O network dependence of optical charge-transfer gaps and spin-pair excitations in single-CuO_2-layer compounds *Phys. Rev.* B **41** 11657–60

[24] Zaanen J and Gunnarsson O 1989 Charged magnetic domain lines and the magnetism of high-Tcoxides *Phys. Rev.* B **40** 7391–4

[25] Anisimov V I, Zaanen J and Andersen O K 1991 Band theory and Mott insulators: Hubbard Uinstead of StonerI *Phys. Rev.* B **44** 943–54

[26] Xu X Q, Mao S N, Jiang W, Peng J L and Greene R L 1996 Oxygen dependence of the transport properties of $Nd_{1.78}Ce_{0.22}CuO4_{\pm\delta}$ *Phys. Rev.* B **53** 871–5

[27] Xiang T, Luo H G, Lu D H, Shen K M and Shen Z X 2009 Intrinsic electron and hole bands in electron-doped cuprate superconductors *Phys. Rev.* B **79** 014524